

Half-life of ^{26}Al

J. H. Thomas, R. L. Rau, R. T. Skelton, and R. W. Kavanagh

Kellogg Radiation Laboratory, California Institute of Technology, Pasadena, California 91125

(Received 17 February 1984)

We have measured the half-life of ^{26}Al because data on ^{21}Ne production rates in meteorites has indicated that the half-life may have been too low by 30–40%. We produced ^{26}Al using the $^{26}\text{Mg}(p,n)^{26}\text{Al}$ reaction on thick natural Mg, the yield being calculated from cross section data. The activity of two such samples was measured with a Ge(Li) detector and the calculated half-life is $t_{1/2} = (7.8 \pm 0.5) \times 10^5$ years, in agreement with the accepted half-life of ^{26}Al : $t_{1/2} = (7.16 \pm 0.32) \times 10^5$ years. Therefore, another explanation must be found for the anomalous ^{21}Ne production rate based on ^{26}Al ages in meteorites.

The accepted half-life of ^{26}Al is based on the work of Rightmire, Kohman, and Hintenberger.¹ They manufactured ^{26}Al at a cyclotron, determined the ^{26}Al content of the sample with a mass spectrometer, and measured the activity of the sample by counting the positrons from the ^{26}Al beta decay in a 4π geiger counter. They calculated a half-life of $(7.4 \pm 0.3) \times 10^5$ years based on the then known properties of the ^{26}Al decay. Later, Samworth, Warburton, and Engelbertink² re-examined the decay scheme of ^{26}Al and recalculated the half-life yielding the currently accepted value of $(7.16 \pm 0.32) \times 10^5$ years.³

^{26}Al is a cosmogenically important isotope because of its convenient half-life and because it is one of several isotopes that are formed in meteorites by cosmic-ray-induced spallation reactions. Kr, Mn, Na, Be and Al are all important examples, although the radioactive and stable isotopes of these elements evolve differently. For example, the ^{26}Al concentration in a meteorite increases with time until an equilibrium is reached between the production rate and the decay rate. ^{21}Ne , on the other hand, is stable and so its concentration builds up linearly with time. The ratio of ^{26}Al to ^{21}Ne concentration is therefore a chronometer and a sensitive indicator of the exposure age of the meteorite⁴ on the million-year time scale.

Conversely, if the exposure age of a meteorite can be determined by one method such as $^{81}\text{Kr}/^{83}\text{Kr}$, then the production rates of other isotopes can be estimated. This was done for ^{21}Ne by Herzog and Anders⁵ using exposure ages determined by the $^{26}\text{Al}/^{21}\text{Ne}$ method on meteorites in which the ^{26}Al had not built up to saturation levels.

Their result gave a ^{21}Ne rate that was higher than expected. Recently, Nishiizumi *et al.*⁶ and Moniot *et al.*⁷ have reviewed the literature concerning the ^{21}Ne production rate problem. (See Table I.) They report that the ^{21}Ne production rate is 0.30×10^{-8} cm³ (STP)/g My based on ^{81}Kr , ^{53}Mn , ^{22}Na , and ^{10}Be , while the production rate based on the ^{26}Al method is 0.45×10^{-8} . Possible explanations for this include a variable cosmic-ray flux or an error in the half-life of ^{26}Al .

We have tested the hypothesis that the accepted half-life is in error. We did so by manufacturing a known amount of ^{26}Al , measuring the sample's decay rate with a Ge(Li) detector, and then calculating the half-life from this information. We avoided the difficulties of mass spectrometry by manufacturing the aluminum via a reaction with a known cross section,⁸ $^{26}\text{Mg}(p,n)^{26}\text{Al}$. The experimental setup is shown schematically in Fig. 1. Two targets of natural magnesium were bombarded with an $E_{\text{lab}} = 5.800$ MeV proton beam. This energy was chosen because it corresponded to the highest energy data point taken by Skelton and Kavanagh⁸ for the $^{26}\text{Mg}(p,n)^{26}\text{Al}$ cross section. The beam energy corresponds to 0.796 MeV excitation energy in ^{26}Al which is between the second and third excited states. Only the ground and the second excited states will contribute to the ^{26}Al ground-state yield because the first excited state beta decays directly to the ground state of ^{26}Mg .

The targets were mounted in a high-vacuum chamber that was separated from the accelerator vacuum by an iso-

TABLE I. A summary of ^{21}Ne production rates.

Method	^{21}Ne production rate [10^{-8} cm ³ (STP) / g My]	Reference
^{26}Al	0.507 ± 0.039	6
^{26}Al	$0.43 - 0.48$	7
^{53}Mn	0.302 ± 0.013	6
^{81}Kr - ^{83}Kr	0.312 ± 0.017	6
^{22}Na - ^{22}Ne	0.292 ± 0.019	6
^{10}Be	0.28 ± 0.02	7

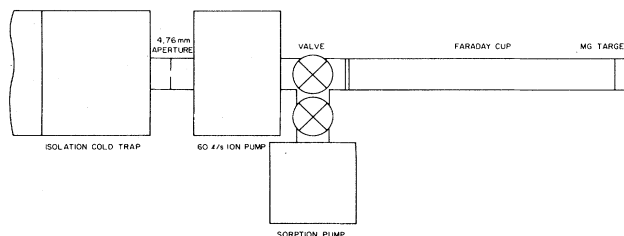


FIG. 1. A schematic representation of the Mg target holder used for the production of ^{26}Al . The 4.76 mm aperture was at a distance of 1.90 meters from the target.

lation cold trap and a 60 l/s ion pump. The vacuum was typically below 1×10^{-7} Torr with beam on the target.

Target number one was manufactured from a solid rod of magnesium by drilling a 1.27 cm hole down through the center of the rod to a depth of 4 cm. The hope was that any ^{26}Al that was sputtered from the target would be trapped by the walls of the hole and then could be removed with an acid etch after the bombardment. A tantalum aperture (0.635 cm diameter) was placed upstream of this target in order to catch any sputtered target material that may emerge from the hole. None was observed via a technique that will be described below.

Target number two was a flat 1.27 cm disk of magnesium. This disk was small enough so that it could be totally dissolved in acid after the bombardment. The target was mounted at the end of a 4 cm long by 1.27 cm diameter monitor tube that was designed to catch sputtered particles from the target. An upper limit to the sputtering yield was easily determined due to the relatively large cross section for $^{25}\text{Mg}(p,\alpha)^{22}\text{Na}$ and due to the short half-life of ^{22}Na . Compared to the ^{22}Na activity of the target the snout collected only enough sputtered particles to account for 0.1% of the total activity and so we assume that a negligible amount of the ^{26}Al was lost via sputtering processes. This result is consistent with the low sputtering yields for proton bombardment of metals, and indeed no damage to the target was visible to the naked eye.

The two targets were cut from a solid magnesium bar of 99.8% purity. The remaining 0.2% impurities gave rise to some bothersome activity in the sample. Principally, so much ^{56}Co was produced via the $^{56}\text{Fe}(p,n)^{56}\text{Co}$ reaction that its gamma ray at 1810 keV obscured the anticipated ^{26}Al signal at 1808 keV. Fortunately, this and other contaminants were easily removed with anion and cation exchange resin techniques.⁹ The procedures we used are outlined below.

Target one was etched in 6N HCl and to this was added 20 mg of Al from a Fischer atomic absorption standard solution. The Al was added as a tracer in order to determine the total yield after all of the chemistry had been completed. Target two was handled similarly except that it was totally dissolved in acid. Ammonium chloride was added to the solutions to inhibit the precipitation of magnesium and then the aluminum was precipitated as the hydroxide by adding ammonium hydroxide. The precipitate was redissolved in 1N HCl and run through a cation exchange column of AG50W-X8, 100-200 mesh, H^+ form. This separated Al from Na and the aluminum was eluted with 10N HCl. The eluate was then passed through an anion exchange column of AG1-X8, 100-200 mesh, Cl^- form. This separated the Al from the Co and the purified Al solution was then packaged in an approximately 2 cm³ cylindrical Plexiglas vial for gamma counting. The resulting spectrum showed that the Co had been reduced to the point that it was indistinguishable from the background, see Fig. 2. The sample was still contaminated with ^{51}Cr but this was deemed to be unimportant due to the low energy (320 keV) of the Cr line.

We detected the 1808 keV gamma transitions resulting from the ^{26}Al ground-state decay with a 100 cm³ Ge(Li)

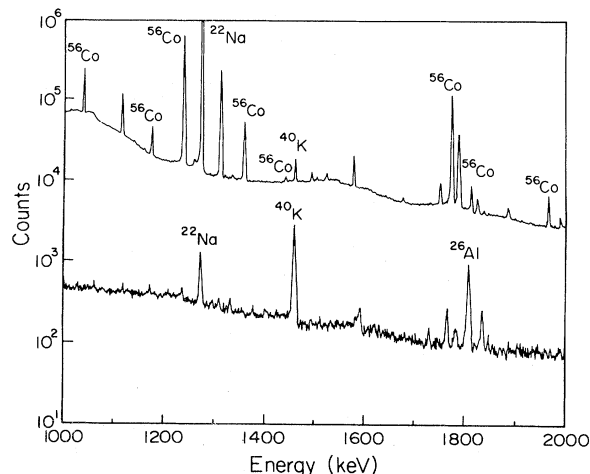


FIG. 2. Ge(Li) spectra of target 1 after proton bombardment (upper) and after chemical processing to eliminate the ^{56}Co lines (lower). The smaller peaks in the lower curve are due to background radiation from ^{226}Ra , ^{214}Bi and the $^{22}\text{Na} + 0.511$ sum peak.

detector. The samples were counted in close proximity to the Ge(Li) and summing corrections were determined by counting a standard sample of $^{26}\text{Al}_2\text{O}_3$ in the same geometry and again in an extended geometry where the summing corrections were negligible. The calibration of the ^{26}Al standard was then checked against a Eu-Sm source purchased from the National Bureau of Standards (NBS No. SRM-4275-164).

The sample vials were then opened and diluted to an aluminum concentration of approximately 200 $\mu\text{g}/\text{ml}$ for atomic absorption analysis (AA). 2 mg/ml of KCl was added to the solutions to enhance the Al signal in the AA. Several further dilutions of the samples were made and then all of the solutions were analyzed via atomic absorption and compared to similar dilutions of the Fischer Al AA standard and to a Caltech Al standard solution. All of the measurements were consistent and they showed no evidence for absorption interferences from other elements. The total Al in each sample was then compared to the amount of ^{27}Al added as a tracer to give us a direct measure of the chemical yield. As can be seen in Table II, a considerable portion of sample one was lost, but sample two was handled much more satisfactorily.

The number of ^{26}Al atoms produced was calculated from the total integrated beam current, the cross-section data of Skelton and Kavanagh,⁸ and the stopping-power compilation of Anderson and Ziegler.¹⁰ The formula used was

$$N_{^{26}\text{Al}} = \frac{N_0 N_p A_{rel}}{A_{nat}} \int \frac{\sigma(E)}{\epsilon} dE,$$

where N_0 is Avogadro's number, N_p is the number of protons incident, A_{rel} is the relative abundance of ^{26}Mg , and A_{nat} is the atomic weight of natural Mg. The integral runs from threshold to the bombarding energy yielding a value of (21.6 ± 1.3) mb MeV with an average stopping power, $\bar{\epsilon}$, of (55.2 ± 0.5) keV cm²/mg. σ refers to the sum of the cross sections to the ground state and second excit-

TABLE II. A summary of the data measured during the course of this work, and our calculations of the half-life of ^{26}Al .

	Sample I	Sample II
Integrated beam current (Coulombs)	1.88 ± 0.08	3.04 ± 0.10
1.808 MeV γ counts	1090 ± 60	3650 ± 75
γ counting time (sec)	1425 839	749 536
Chemical efficiency (%)	23.0 ± 0.7	93.0 ± 1.5
Ge(Li) efficiency (%)	0.92 ± 0.03	0.92 ± 0.03
Yield of ^{26}Al atoms	$(1.27 \pm 0.09) \times 10^{13}$	$(2.05 \pm 0.14) \times 10^{13}$
Half-life (yr)	$(7.7 \pm 0.7) \times 10^5$	$(7.9 \pm 0.6) \times 10^5$

ed state of ^{26}Al . The other relevant experimental parameters are summarized in Table II. The half-life calculated is $(7.8 \pm 0.5) \times 10^5$ years. This value is consistent with the currently accepted half-life of ^{26}Al and therefore it appears that an error in the half-life is not the cause of the ^{21}Ne production rate problem.

During the course of this work we learned of two other experiments that were designed to measure the half-life of ^{26}Al . One is being done at Los Alamos,¹¹ where they have measured the activity of a sample of ^{26}Al with a Ge(Li) detector. The sample had previously been analyzed by conventional mass spectrometry to determine the ^{26}Al content. They calculate a half-life of $(7.0 \pm 0.4) \times 10^5$

years. Another group, at Pennsylvania, has done accelerator-based mass spectrometry¹² on an enriched sample of ^{26}Al for which the activity of the sample was already known. They calculate a half-life of $(7.0 \pm 0.6) \times 10^5$ years.

We are grateful for the advice and assistance received from Dr. Henry Ngo on the chemical separation procedures. We are also grateful for the long-term loan of a data-acquisition system owned by the Inter-American Tropical Tuna Commission. This work was supported in part by the National Science Foundation under Grants Nos. PHY79-23638 and PHY82-15500.

¹R. A. Rightmire, T. P. Kohman, and H. Hintenberger, *Z. Naturforsch.* **13a**, 847 (1958).

²E. A. Samworth, E. K. Warburton, and G. A. P. Engelbertink, *Phys. Rev. C* **5**, 138 (1972).

³C. M. Lederer and V. S. Shirley, *Table of Isotopes*, Seventh Edition (Wiley, New York, 1978).

⁴M. E. Lipshutz, P. Signer, and E. Anders, *J. Geophys. Res.* **70**, 1473 (1965).

⁵G. F. Herzog and E. Anders, *Geochim. Cosmochim. Acta* **35**, 605 (1971).

⁶K. Nishiizumi, S. Regnier, and K. Marti, *EPSL* **50**, 156 (1980).

⁷R. K. Moniot *et al.*, *Geochim. Cosmochim. Acta* (in press).

⁸R. T. Skelton, R. W. Kavanagh, and D. G. Sargood, *Astrophys. J.* **271**, 404 (1983); and (unpublished).

⁹J. E. Lewis, *The Radiochemistry of Aluminum and Gallium, NAS-NS 3032* (National Research Council, Washington, D.C., 1961).

¹⁰H. H. Anderson and J. F. Ziegler, *Hydrogen Stopping Powers and Ranges in All Elements* (Pergamon, New York, 1977).

¹¹T. L. Norris *et al.*, *Abstracts of the 14th Lunar Science Conference* (Lunar and Planetary Institute, Texas, 1983), p. 568.

¹²R. Middleton, J. Klein, G. M. Raisbeck, and F. Yiou, submitted to *Nucl. Instrum. Methods*.